Heliyon 9 (2023) e19817

Contents lists available at ScienceDirect

Heliyon

journal homepage: www.cell.com/heliyon

(−)-Guaiol inhibit epithelial-mesenchymal transition in lung cancer via suppressing M2 macrophages mediated STAT3 signaling pathway

Yajuan Cao [a,1], Yonghui Wu [a,b,1], Hongbin Tu [a,1], Zhan Gu [a], Fengzhi Yu [a], Weiling Huang [c], Liping Shen [d], Lixin Wang [a,*], Yan Li [e,**]

[a] Department of Integrated Traditional Chinese and Western Medicine, Shanghai Pulmonary Hospital, School of Medicine, Tongji University, 507 Zhengmin Road, Yangpu District, Shanghai 200433, China
[b] Shanghai University of Traditional Chinese Medicine, Shanghai 201203, China
[c] Shanghai Jing 'an District Hospital of Traditional Chinese Medicine, Shanghai 200072, China
[d] LongHua Hospital Shanghai University of Traditional Chinese Medicine, Shanghai 200032, China
[e] Shanghai Municipal Hospital of Traditional Chinese Medicine, Shanghai University of Traditional Chinese Medicine, Shanghai 200071, China

ARTICLE INFO

Keywords:
(−)-Guaiol
Macrophage
Lung cancer
Interleukin 10
STAT3

ABSTRACT

In the context of cancer expansion, epithelial-mesenchymal transition (EMT) plays an essential role in driving invasion and metastasis potential of cancer cells. Tumor-associated macrophages (TAMs)-derived factors involved in the initiation and progression of EMT. We assess the role of M2 macrophage in suppressing lung tumors of a natural compound (−)-Guaiol by using macrophage depleted model. Bone marrow-derived monocytes (BMDMs) were extracted and induced to M2-like phenotype in vitro. The co-culture of M2 macrophage and lung cancer cells was established to observe that inhibition of lung tumor growth by (−)-Guaiol requires presence of macrophages. This suppressed effect of (−)-Guaiol was alleviated when mice macrophage was depleted. The expression of M2-like macrophages was strongly reduced by (−)-Guaiol treated mice, but not the changes of M1-like macrophages. In vitro studies, we demonstrated that (−)-Guaiol suppressed M2 polarization of BMDMs, as well as migration, invasion, and EMT of lung cancer cells in co-culture. M2 macrophage-derived interleukin 10 (IL-10) was investigated as a critical signaling molecule between M2 macrophage and lung cancer cells. We have also verified that the mechanism of (−)-Guaiol inhibiting the EMT process of lung cancer is related to the activation of IL-10-mediated signal transducer and activator of transcription 3 (STAT3). These results suggested that the suppressive effect role of (−)-Guaiol in M2 macrophage promoting EMT of lung cancer, which was associated with inhibition of IL-10 mediated STAT3 signaling pathway.

1. Introduction

Lung cancer remains the leading cause of cancer incidence and mortality worldwide, representing close to 1 in 5 (18.4%) cancer

* Corresponding author.
** Corresponding author.
E-mail addresses: 1701005@tongji.edu.cn (L. Wang), yan.xiaotian@shutcm.edu.cn (Y. Li).
[1] These authors contributed equally to this work.

https://doi.org/10.1016/j.heliyon.2023.e19817
Received 26 June 2023; Received in revised form 29 August 2023; Accepted 1 September 2023
Available online 7 September 2023

deaths [1,2]. Most patients often present an advanced disease stage when detected at initial diagnosis. Tumor metastasis, as a hallmark of cancer [3], has become the main reason to refrain from the improvement of the curative effect and result in most lung cancer-associated deaths.

In the context of cancer expansion, tumor invasion and distant metastasis is a multi-step, multi-factor participation process, which is often portrayed as "invasion-metastasis cascade" [4]. As well as we know, the neoplastic cells are in an epithelial-like state in the early stage of tumors, and gradually acquire mesenchymal characteristics at progression proceeds. It was named epithelial-mesenchymal transition (EMT). EMT plays an important role in driving the multiple steps of "invasion-metastasis cascade". Activation of EMT confers enhanced invasion and metastasis potential of cancer cells [5], and is related to the poor prognosis of tumors, including lung, pancreatic, breast, hepatocellular and colorectal cancer [6–9].

Tumor growth and metastasis are closely associated with the tumor microenvironment [10]. Macrophages are the main component of immune cells in the micro-environment [11]. Due to the remarkable plasticity and capability to secrete various cytokines, chemokines, growth factors and enzymes, they play an essential role in regulating the homeostasis of the micro-environment [12]. Under local micro-environmental conditions, macrophages acquire distinct phenotypes and polarize into either "classical activated" pro-informatory property (M1) or "alternatively activated" anti-inflammatory property (M2) [13]. Tumor-associated macrophages (TAMs) are characterization of M2 phenotype whose functions have been shown to promote cancer progression, angiogenesis, invasion and metastasis, as well as immunosuppression [14].

Accumulate evidence indicates that TAMs play a crucial part in the regulation of EMT in tumors. TAMs-derived factors involved in the initiation and progression of EMT [14]. In our previous studies, M2 macrophage producing MMPs and VEGF significantly promoted tumor invasion and metastasis in non-small cell lung cancer (NSCLC), whereas remodifying of TAM away from M2-like, towards M1-like phenotype, suppressed lung cancer cell aggressive behaviors [15]. In addition, our studies demonstrated (−)-Guaiol, a component of many medicinal plants [16], has anti-tumor activity in NSCLC cells [17,18]. The results suggested us to take a new insight into whether (−)-Guaiol for possibility of targeting TAMs as a potential therapeutic strategy in lung cancer.

The present study aims to investigate the impact of (−)-Guaiol on regulation of TAMs. Based on the close relevance between TAMs and EMT in lung cancer, we also preliminarily explored the role of (−)-Guaiol underlying TAMs-derived EMT in lung cancer.

2. Materials and methods

2.1. Bioinformatics analysis

Two mRNA expression datasets of M2 macrophages, GSE5099 and GSE57614, were downloaded from the GEO database (https://www.ncbi.nlm.nih.gov/geo/). mRNA profile of lung cancer was obtained from The Cancer Genome Atlas (TCGA, https://cancergenome.nih.gov/) database. The differential expression genes (DEGs) were screened by GeneSpring GX 12.5 software (Agilent Technologies, Santa Clara, CA, US), the detailed screening criteria were shown in our previous studies [19]. Overlapped between M2 macrophages and lung cancer DEGs were extracted and performed a Gene Ontology (GO) analysis and Kyoto Encyclopedia of Genes and Genomes (KEGG) enrichment analysis by gene set enrichment analysis (GSEA) (version 3.0, http://software.broadinstitute.org/gsea/) [20,21].

2.2. Animals studies

Following the Guide for the Care and Use of Laboratory Animals of the National Institutes of Health, and approval by the Committee on the Ethics of Animal Experiments of Shanghai University of Traditional Chinese Medicine. Animals used were acquired from the China Science Academy (Shanghai, China) that carries the C57BL/6 background, kept under specific-pathogen-free (SPF) conditions.

1×10^6 LLC cells were injected subcutaneously to the flanks of C57BL/6 mice. Clodronate liposomes (www.clodronateliposomes.org, Netherland) was started 2 days before LLC injection and followed by sustained intraperitoneal administration every 4th day. After one week of LLC injection, the subcutaneous nodule was observed. Given (−)-Guaiol (8 mg/kg) or an equal size of PBS every 2 days ($n = 4$). Tumor growth was monitored every 3 days for 3 weeks.

2.3. Cell culture

Lewis lung cancer (LLC) cells were acquired from the Cell Bank of the China Science Academy (Shanghai, China) and cultured in complete DMEM medium (supplemented with 10% Fetal Bovine Serum (Gibco, Australia) and 1% Penn/Strep).

Bone marrow-derived macrophages (BMDMs) were collected from femurs and tibias of 6–8 week-old C57Bl/6 mice [22]. BMDMs were plated into a 6 cm culture dish and treated with 10 ng/ml murine M-CSF (Peprotech, USA) for 7 days to allow differentiation of monocytes into macrophages. Macrophages were exposed to 20 ng/ml murine recombination IL-4 (R&D, USA) to polarize to M2-like macrophages. M2-like macrophages were harvested and used for next co-culture experiments.

2.4. Co-culture of macrophages and LLC cells

The macrophage-conditioned medium (CM) was harvested after the M2 macrophages incubated with (−)-Guaiol for 24 h. The LLC cells were exposed in 50% CM (1:2 dilution with complete DMEM) and incubated for 24 h.

2.5. Cell proliferation, invasion and migration assay

Cell proliferation activity was detected with CCK-8 assay. Briefly, 5×10^3 per well cells were seeded in the 96-well culture plates overnight. Cells were exposed in CCK-8 after treating with (−)-Guaiol for 24 h. Absorbance was obtained by a Microplate Reader (Thermo Scientific, USA) at a wavelength of 450 nm. IC 50 value was calculated with Graphpad Prism software.

Cells invasion were performed in a 24-well transwell system (Corning, USA) fitted with a polyethylene terephthalate filter membrane with 8 μm pore size. The upper chamber was provided with Matrigel (Millipore, Bedford, MA). Either control or co-culture CM was introduced to the lower chamber and LLC cells (4×10^4) were placed into the upper chamber. 48 h later, the traversed cells were fixed, stained and calculated.

Cells migration were carried out with a wound-healing assay. Cells were implanted into 6-well culture plates. A "wound" was scratched on the monolayer with 10 μL micropipette. The migration of samples was captured with microscope at the beginning and 24 h later, respectively.

2.6. Flow cytometry analysis

BMDMs were collected and washed twice with PBS. Spleen and tumor tissues were minced and dissociated with Dissociation kit (Miltenyi, Germany), according to manufacturer's instructions. The pellets were re-suspended in DMEM, and then monocytes were isolated according to density gradient centrifugation on Percoll. 1×10^6 cells were stained with anti-mouse fluorochrome-labeled antibodies (F4/80-FITC, CD206-PE, all PeproTech) for 15 min at room temperature. After washing steps, cells were identified with flow cytometer (BECKMAN). Data were analyzed with FlowJo software.

2.7. Quantitative real-time polymerase chain reaction

Total RNA was extracted with TRIzol reagent (Invitrogen). cDNA was synthesized with PrimeScript RT Reagent kit (TaKaRa). Real-time PCR was carried out with SYBR Green Master Mix (TaKaRa, Japan) on a QuantStudio 6 Flex real-time PCR system (Thermo Fisher, USA). The murine-GAPDH serves as endogenous control. All mRNA levels were normalized to GAPDH and quantified with $2^{-\triangle\triangle CT}$. Data were analyzed with GraphPad prism. Primer sequences were attached in Table S1.

2.8. Western blot analysis

Total protein was extracted with RIPA lysis buffer supplemented with proteinase inhibitor and phosphatase inhibitor. Protein concentrations were measured using the BCA protein assay kit (Thermo Fisher Scientific, USA). Equivalent amounts of protein were resolved on SDS-PAGE gels and blotted onto polyvinylidene difluoride membranes. After blocking non-specific binding sites with blocking solution (1 × TBS, 0.1% Tween 20, and 5% bovine serum albumin) at room temperature for 2 h. The membranes were incubated with CD206, E-cadherin, N-cadherin, Vimentin, STAT3, p-STAT3, IL-10 (all Cell Signaling Technology, USA), and GAPDH (Abcam, USA) overnight at 4 °C. The membranes were incubated with HRP-conjugated secondary antibodies (Cell signaling Technology, USA) after adequate washing with TBST for 1 h at room temperature. Finally, the blots were subjected to chemiluminescence analysis (BIO-RAD, USA).

2.9. Enzyme-linked immunosorbent assay

IL-10 levels were quantified in peripheral blood of mice and conditioned medium with the Mouse IL-10 ELISA Kit (R&D Systems) according to the manufacturer's instruction.

2.10. Statistics analysis

Data were presented as mean ± SD. The statistical differences were assessed with Student's T-test or two-way ANOVA. P value < 0.05 was considered as statistically significant.

3. Results

3.1. M2 macrophages promotes lung cancer expansion by secreting cytokines

There is communication between macrophages and tumors. To predict the mechanism of M2 macrophages promotes lung cancer expansion. We identified the DEGs of M2 macrophages by analyzing the transcriptome of M0 and M2 macrophages after 24-h-polarization in GEO databases and the DEGs of lung cancer in TCGA databases, respectively.

We identified 1998 DEGs of M2 macrophage (715 upregulated and 844 downregulated genes) and 4456 DEGs of lung cancer (1966 upregulated and 2490 downregulated genes). A total of 139 overlapped genes were extracted between M2 macrophage and lung cancer, including 48 upregulated and 91 downregulated genes. As shown in Venn diagram (Fig. 1A and B). As we known M2 macrophage facilitates tumor progression, 48 upregulated genes were performed an enrichment analysis by GSEA. The TOP 15 GO and TOP 10 KEGG terms were exhibited in Fig. 1C and D. GO analysis revealed that biological process (BP) was significantly enriched in

Response to external stimulus, cellular component (CC) was distinctly classified in Extracellular space, and molecular functions (MF) was mainly associated with Cytokine activity and Cytokine receptor binding. The most enrichment term of KEGG pathway was Cytokine-cytokine receptor interaction. Briefly, enrichment analysis suggested that M2-derived cytokines mediated the cytokine-cytokine receptor interaction signaling pathway as the likely mechanism by which M2 macrophages acted on lung cancer.

3.2. Inhibition of lung cancer growth by (−)-Guaiol requires presence of macrophages in vivo

To assess the critical role of macrophage in (−)-Guaiol inhibiting lung cancer growth, we used a subcutaneously injected mice model of Lewis Lung carcinomas (LLC) tumor cells, where macrophages were depleted with clodronate liposome (CL), as shown in Fig. 2A. Macrophages depletion inhibited the lung tumor growth was observed. Meanwhile, 21 days intraperitoneal injection of (−)-Guaiol could inhibit lung tumor growth in PBS Liposome (PBSL) mice model. However, the effect of (−)-Guaiol in further inhibiting tumor growth was not observed in the macrophage depletion mice model (Fig. 2B). An obvious difference was uncovered in mice without macrophage depletion, the volume of primary tumors in (−)-Guaiol treated group were smaller than control, while the effects of (−)-Guaiol were not revealed in macrophage depletion mice (Fig. 2C). The tumor was peeled off and weighted on the experimental endpoint. Consistent with these observations, the tumor weight in (−)-Guaiol treated group was significantly lower (Fig. 2D). The body weight of mice was monitored biweekly. Our research findings indicated that, following a 21-day treatment period, no noteworthy variance in body weight was observed across the different groups. (Fig. 2E).

To further test the role of macrophage polarization in lung cancer progresses, we observed the M2-like polarization macrophage expression in tumor and spleen, respectively. In corroboration, a reduced number of macrophages of the tumor and spleen microenvironment were measured by flow cytometry. The macrophage depletion mainly reflected in M2-like polarization macrophage decreasing. Interestingly, we found that the expression of M2-like macrophages was strongly reduced by (−)-Guaiol treated mice. The same tendency was observed in the tumor (Fig. 2F) and spleen (Fig. 2G) microenvironment of (−)-Guaiol treated mice.

Our results revealed that macrophages play an essential role in lung cancer-promoting. Inhibition of subcutaneous lung cancer growth by (−)-Guaiol requires the presence of macrophages. This effect of (−)-Guaiol in suppressing tumor growth reflected in suppressing M2-like macrophages in the tumor and spleen microenvironment.

3.3. M2-like macrophages polarization and identification in vitro

To explore the relationship between TAM and lung cancer cells, we established a M2-like macrophages model in vitro. Macrophages were generated from mouse bone marrow using macrophage colony-stimulating factor (M-GSF) for 7 days to allow differentiation of monocytes into macrophages, then macrophages were exposed in IL-4 to polarize an M2 phenotype (Fig. S).

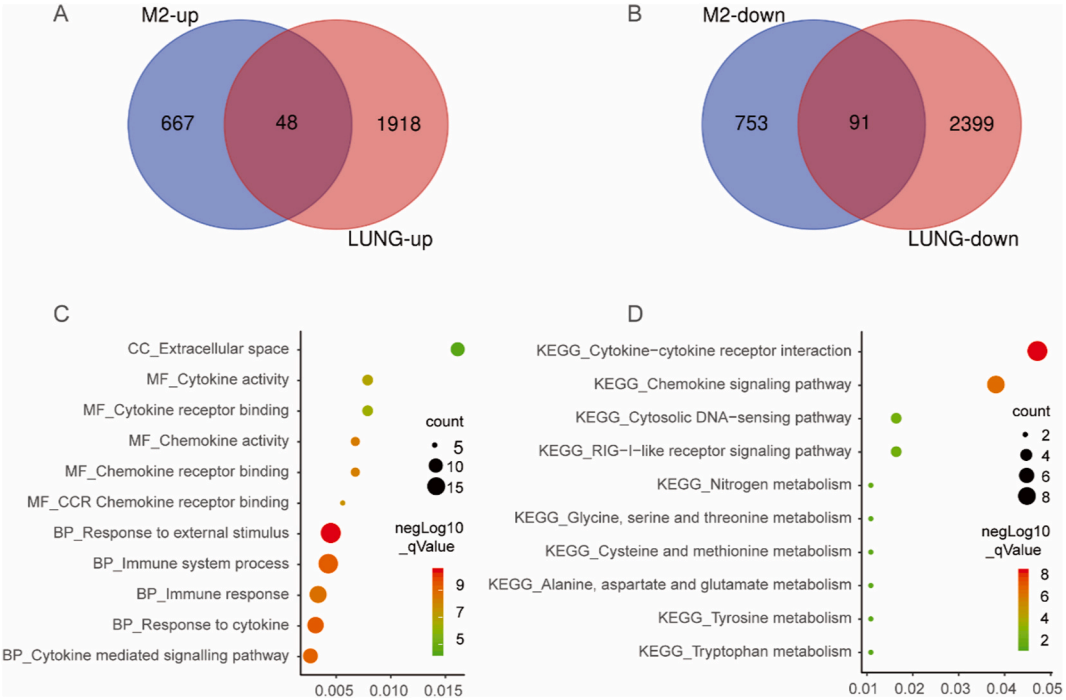

Fig. 1. M2 macrophage promotes lung cancer expansion by secreting cytokines. (A) Venn diagram of 48 overlapping upregulated differential expression genes (DEGs) and (B) 91 overlapping downregulated DEGs between M2 macrophage and lung cancer. (C) GO enrichment analysis and (D) pathway enrichment analysis of 48 overlapping upregulated DEGs.

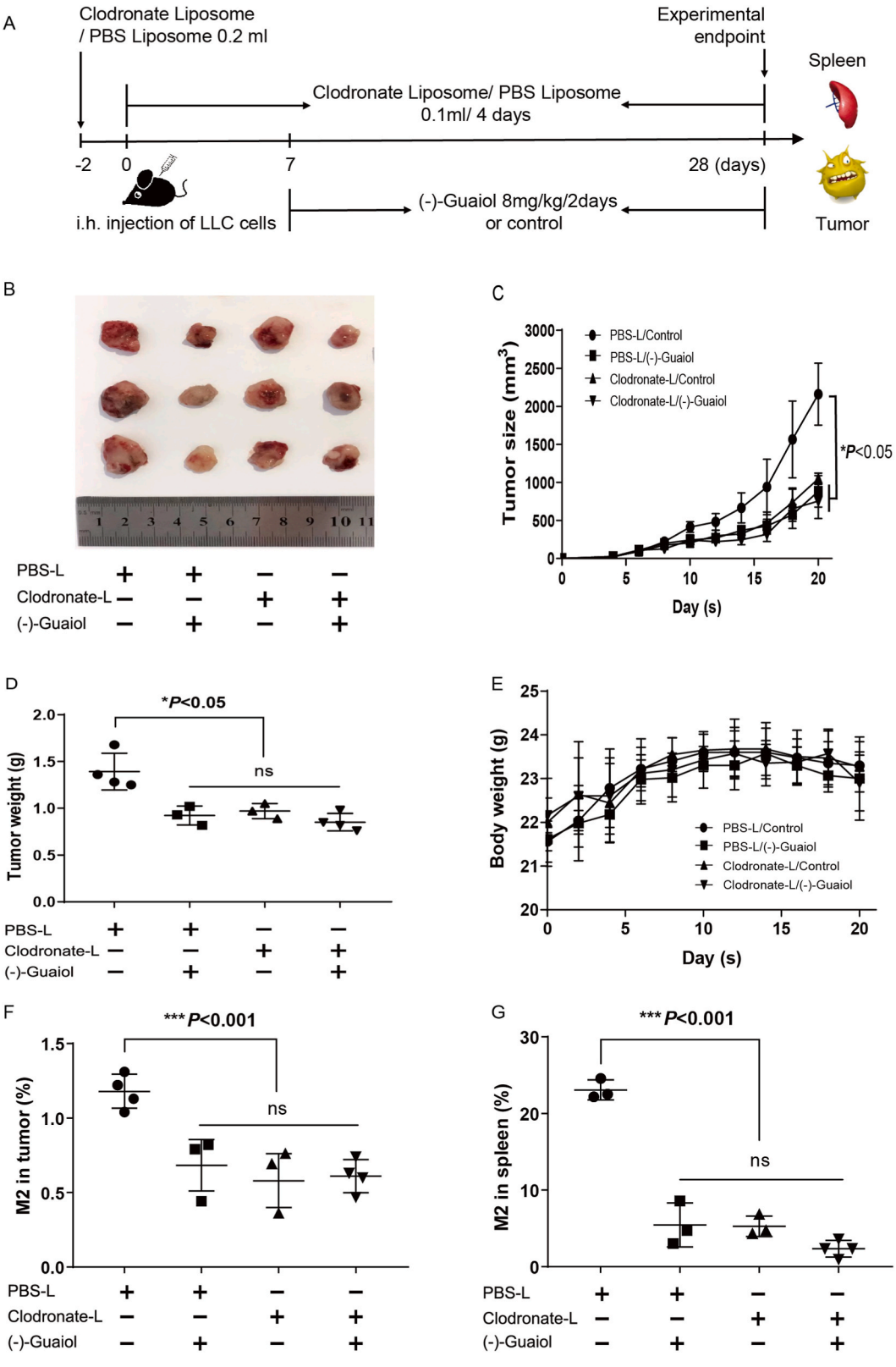

(caption on next page)

Fig. 2. Inhibition of lung cancer growth by (−)-Guaiol requires presence of macrophages in vivo. (A) Schematic design of animal experiments. (B) Images of xenograft tumors in C57BL/6 mice after subcutaneous inoculation of Lewis lung carcinoma (LLC) cells. (C) The tumor size and (D) weight of xenograft tumors in each group at the experimental endpoint. Compared with PBS liposome group without (−)-Guaiol treatment, tumor size and weight in mice with (−)-Guaiol treatment was inhibited obviously (*$P < 0.05$). While the effects of (−)-Guaiol were not revealed in macrophage depletion mice. (E) Body weight of mice was no significant difference between groups after 21 days treatment. The amount of M2-like polarization macrophage in the (F) tumor and (G) spleen microenvironment were measured by flow cytometry. Compared with PBS liposome group without (−)-Guaiol treatment, the expression of M2-like macrophage was strongly reduced by (−)-Guaiol treated (***$P < 0.001$). Data were represented as means ± STD.

Morphological characterization of macrophages and IL-4 derived macrophages was captured by microscopy. It was shown that after 24H of differentiation with IL-4, the macrophages appear fusiform and extend a large number of pseudopods (Fig. 3A). Significantly high expression of CD206, M2 phenotype surface marker, was detected using flow cytometry (Fig. 3B and C) and Western blot (Fig. 3D and E) in the IL-4 derived macrophages. Meanwhile, we observed a remarkably upregulated mRNA of Arginase-1 and anti-inflammatory genes (IL-10 and IL-13), as shown in Fig. 3F.

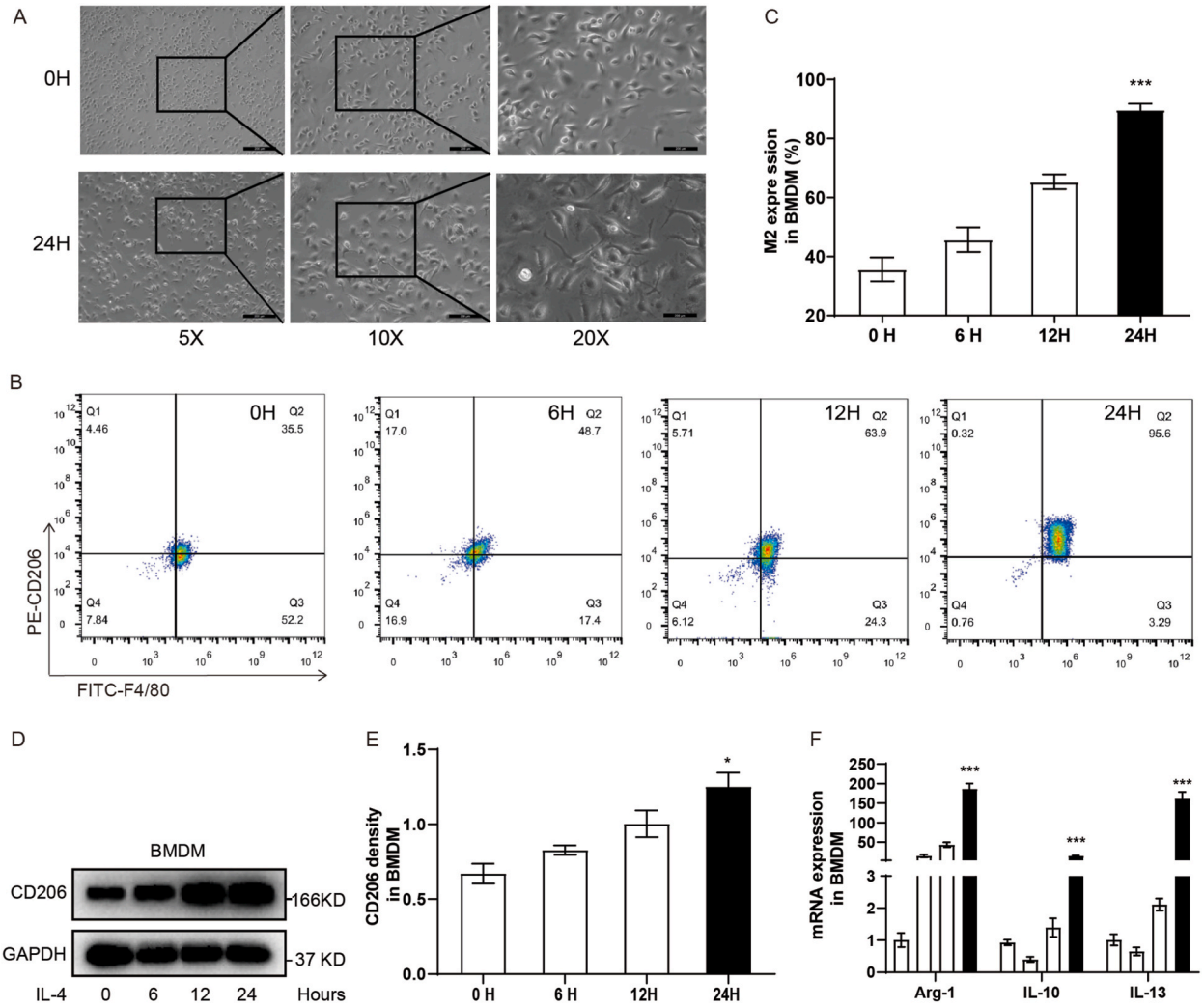

Fig. 3. M2-like macrophages polarization and identification in vitro. (A) Representative pictures of macrophages and IL-4 derived macrophages at 0H and 24H. (B) M2 phenotype surface marker was detected at 0H, 6H, 12H and 24H according to flow cytometry. (C) CD206 and F4/80 were used to co-stain to identify differentiated BMDM population. Compared with 0H, statistical analysis of M2-like macrophage at 24H had higher expression of CD206 (***P < 0.001). (D) IL-4 induced CD206 protein expression at 0H, 6H, 12H and 24H using Western blot assay. (E) Compared with 0H, statistical analysis of M2-like macrophage at 24H had higher expression of CD206 protein (*P < 0.05). (F) RNA from BMDMs was extracted and expression of Arginase1 (Arg1), IL-10 and IL-13 (M2-like macrophage markers) was calculated by quantitative real-time PCR. Compared with 0H, statistical analysis of M2-like macrophage markers at 24H had higher expression (***P < 0.001). Data were represented as means ± STD. Each group was performed with three biological replicates. All experiments were performed with three biological replicates.

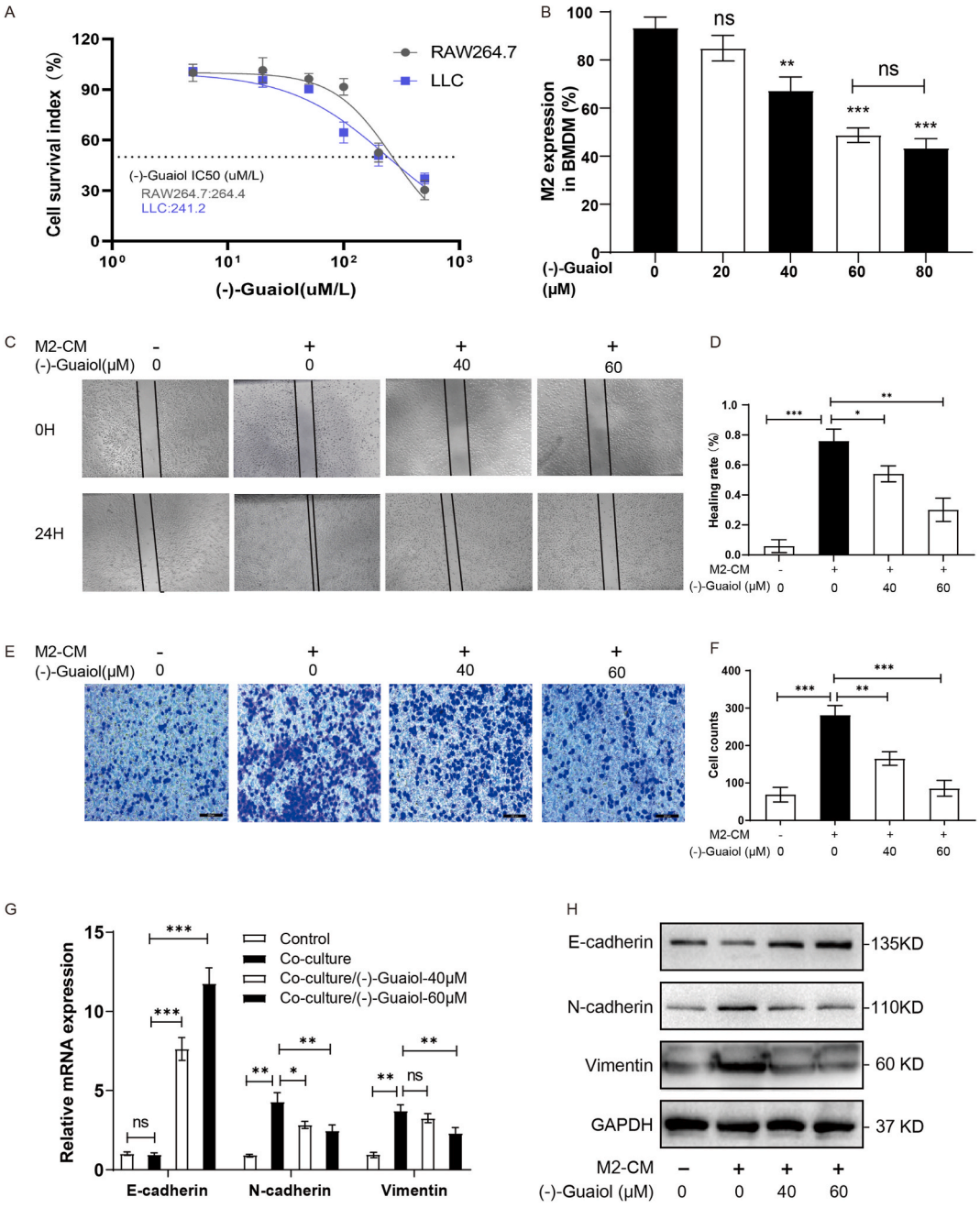

Fig. 4. (−)-Guaiol suppresses M2 macrophages in vitro, and inhibits migration, invasion, and EMT of lung cancer cells in co-culture. (A)Cell survival analysis of M2 macrophages and Lewis lung carcinoma (LLC) cells treated with different doses of (−)-Guaiol using CCK8 assays. (−)-Guaiol abrogated the growth of M2 macrophages and LLC cells. IC50 values were 264.4 μM and 241.2 μM, respectively. (B) (−)-Guaiol treatment resulted in decreasing of M2-like macrophage. M2 macrophages were subjected to different gradients of (−)-Guaiol for 24 H. Compared with 0 μM, it was observed that 40 μM, 60 μM and 80 μM (−)-Guaiol lowered CD206 expression at the surface of M2-like macrophage significantly at different extent. Meanwhile, it seemed that 60 μM was the most appropriate concentration (***$P < 0.001$). Exposing LLC cells in the macrophage-derived conditioned media (CM), which intervened from (−)-Guaiol. (C–D) Wound-healing assay was used to record the migration of LLC cells in the co-culture system. 60 μM (−)-Guaiol treatment resulted in significantly decreasing the LLC cells migration (**$P < 0.01$). (E–F) LLC cells invasion were performed in a 24-well transwell system. Consistent with migration, 60 μM (−)-Guaiol disrupted the invasion of LLC cells (***$P < 0.001$). (G) mRNA levels of E-cadherin, N-cadherin and Vimentin of LLC cells in co-culture system were detected by RT-qPCR. 60 μM (−)-Guaiol treatment resulted in observably down-regulating the mRNA expression of N-cadherin and Vimentin (**$P < 0.01$) and up-regulating the mRNA expression of E-cadherin (***$P < 0.001$). (H) Western blot analysis of E-cadherin, Vimentin and N-cadherin protein expression of LLC cells in co-culture system. Data from three independent experiments were represented as means ± STD and subjected to ANOVA tests, respectively. All experiments were performed with three biological replicates.

The above results suggested that macrophages are prone to M2 phenotype after IL-4 derived 24H.

3.4. (−)-Guaiol suppresses M2 macrophages in vitro, and inhibits migration, invasion, and EMT of lung cancer cells in co-culture

To probe the biological role of (−)-Guaiol regulating macrophage in vitro, we exposed M2 macrophages and LLC to (−)-Guaiol treatment media at various concentration gradients. In the first step, we conducted independent CCK-8 experiments to evaluate the proliferation of M2 macrophages and LLC cells separately. IC 50 value of (−)-Guaiol works was calculated. (−)-Guaiol could abrogate the growth of M2 macrophage and LLC with IC 50 values 264.4 μM and 241.2 μM (Fig. 4A). Afterward, M2 macrophages were detected using the classic biomarker CD206 in flow cytometry [23,24]. Interestingly, we found that after 24H of treatment with (−)-Guaiol keep macrophage away from CD206 expression significantly. It seemed that 60 μM was the most appropriate concentration (Fig. 4B). Consistent observations were traced through the microscope. A large number of M2 phenotype was reshaped into the morphology of macrophage when exposed in 60 μM (−)-Guaiol (Fig. SB). In our previously reported that 100 μM (−)-Guaiol induces lung cancer cell apoptosis [25]. In this study we showed that 60uM (−)-Guaiol does not induce apoptosis of lung cancer cells in the presence and absence of M2 macrophages (Fig. SC). Therefore, 60 μM (−)-Guaiol was employed in the next study. It was relative safety with no significant toxicity to both macrophages and LLC cells. The above findings confirmed (−)-Guaiol could facilitate the remodeling of M2 phenotype to macrophage in vitro.

To evaluate the role of (−)-Guaiol suppresses the expansion of lung cancer cells by decreasing M2 macrophages polarization, we modeled a co-culture of M2 macrophages and lung cancer cells (M2/LLC). As shown in Fig. SD, exposing LLC in the macrophage-derived conditioned media (CM), which intervened from (−)-Guaiol. We monitored the migration and invasion of LLC cells in the co-culture system. As we knew, M2 macrophage accelerates lung cancer cell progression. Consistent with the report, we found that LLC migration was enhanced by M2-derived CM. Importantly, (−)-Guaiol significantly decreased the LLC migration in co-culture (Fig. 4C and D). Consistent with migration, M2-derived CM could more increase LLC invasion than macrophage-derived CM, and (−)-Guaiol

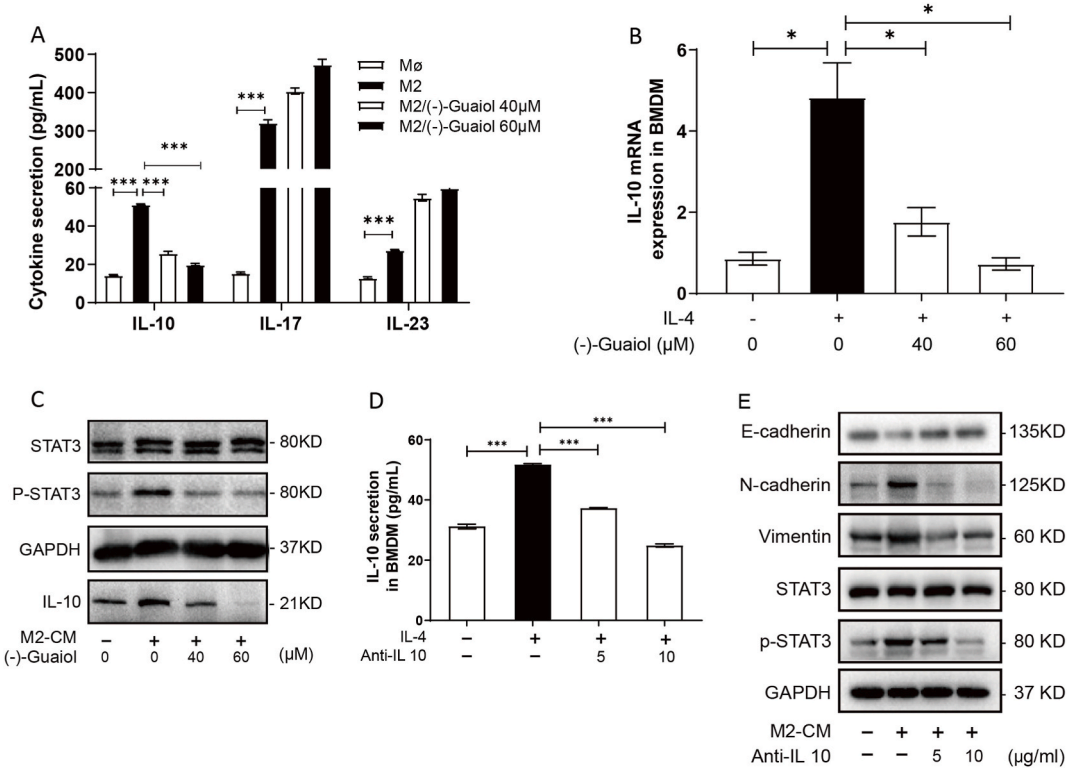

Fig. 5. (−)-Guaiol inhibits STAT3 activation in co-culture, IL-10 is a critical signaling molecule. (A) Cytokines concentration of IL-10, IL-17 and IL-23 in cultured M2 supernatant (M2-CM) was determined with Enzyme-linked immunosorbent assay (ELISA). (−)-Guaiol treatment induced lowered secretion of IL-10 (***$P < 0.001$). Cytokines level was expressed as pg/ml ± STD. (B) mRNA expression of IL-10 from M2 macrophages was calculated by quantitative real-time PCR. It was also down-regulated by (−)-Guaiol-treated (*$P < 0.05$). Data were represented as means ± STD. (C) To unravel the mechanism driving regulation of IL-10, we detected STAT3 activation in LLC with Western blot assay. IL-10 and STAT3 phosphorylation was stimulated in co-culture CM. meanwhile, (−)-Guaiol could suppress the IL-10 and STAT3 phosphorylation in co-culture. (D) We used ELISA to detect that IL-10 secretion in M2-CM was significantly decreased by IL-10 antagonist (anti-IL 10, AS 101, ***$P < 0.001$). Data was expressed as pg/ml ± STD. (E) To further validate the role of IL-10/STAT3 in (−)-Guaiol inhibits lung cancer cells EMT process in co-culture. IL-10 antagonist (anti-IL 10, AS 101) was instead of (−)-Guaiol. Similar suppression of STAT3 phosphorylation and EMT process was observed in LLC with Western blot assay. All experiments were performed with three biological replicates.

disrupted the invasion of LLC in co-culture (Fig. 4E and F).

E-cadherin, N-cadherin and Vimentin serve as biomarkers of EMT. We next assessed the effect of (−)-Guaiol on EMT of lung cancer cells in co-culture. As shown in Fig. 4G, mRNA levels of E-cadherin, N-cadherin and Vimentin were up-regulated after co-culture in LLC compared with control. At the same time, (−)-Guaiol could observably down-regulate the mRNA expression in LLC of E-cadherin, N-cadherin and Vimentin in co-culture. Moreover, a similar effect of (−)-Guaiol was observed when we detected with Western blot (Fig. 4H), EMT process was weakened in co-culture.

These results demonstrate that (−)-Guaiol could suppress migration, invasion and EMT in co-culture, to a certain extent, through inhibiting M2-like macrophage activation.

3.5. (−)-Guaiol inhibits STAT3 activation in co-culture, IL-10 is a critical signaling molecule

The function of macrophages is reflected in the secreted cytokines. We proposed a hypothesis, (−)-Guaiol disturbs the soluble factors that communication between macrophages and lung cancer cells. To verify this hypothesis, we screened secreted mediators in co-culture with ELISA.

We found three cytokines (IL-10, IL-17, IL-23) to be highly expressed in co-culture CM. Notably, (−)-Guaiol significantly decreased IL-10, but not IL-17 and IL-23 (Fig. 5A). mRNA expression of IL-10 was also substantially down-regulated by (−)-Guaiol in co-culture (Fig. 5B). Indicating IL-10 was a critical signaling molecule between macrophages and lung cancer cells for the anti-tumor effect of (−)-Guaiol [26]. STAT3 plays an important role in cytokine activation and EMT [27]. To unravel the mechanism driving regulation of IL-10, we detected STAT3 activation in LLC. As demonstrated in Fig. 5C. STAT3 phosphorylation was stimulated in co-culture CM. meanwhile, (−)-Guaiol could suppress the STAT3 phosphorylation in co-culture. To further validate the role of IL-10/STAT3 in (−)-Guaiol inhibits lung cancer cells EMT process in co-culture. IL-10 antagonist (AS 101) was instead of (−)-Guaiol. IL-10 secretion

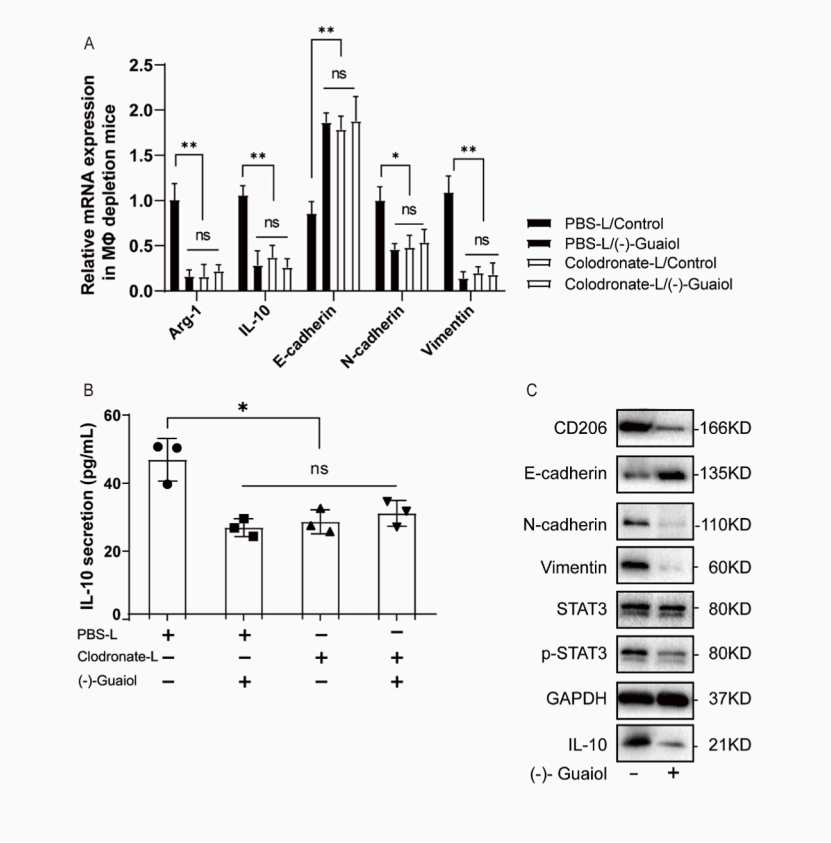

Fig. 6. (−)-Guaiol inhibits lung cancer EMT and IL-10 mediated STAT3 activation in vivo. (A) RNA from xenograft tissue was extracted and expression of Arg-1, IL-10 and EMT markers were calculated by quantitative real-time PCR. (−)-Guaiol significantly suppressed Arg-1, IL-10 and EMT mRNA levels in mice without macrophage depletion, while the effects were partially or not compromised in macrophage depletion mice (* all $P < 0.05$). Data were represented as means ± STD. (B) The levels of IL-10 secretion in peripheral blood of mice were measured with ELISA. (−)-Guaiol substantially decreased IL-10 secretion in mice without macrophage depletion but not in the macrophage depletion mice (*$P < 0.05$). Data was expressed as pg/ml ± STD. (C) We verified EMT and STAT3 activation in mice without macrophage depletion with Western blot assay. (−)-Guaiol weakened the EMT process and STAT3 phosphorylation compared with control. Moreover, the expression of CD206 and IL-10 as well as refrained by (−)-Guaiol.

was obviously decreased by AS 101 in co-culture CM (Fig. 5D). Similar suppression of STAT3 phosphorylation and EMT process was observed in LLC (Fig. 5E). Taken together, suggesting that (−)-Guaiol can inhibit lung cancer cell EMT through suppressing M2 macrophages produce IL-10 mediated STAT3 activation.

3.6. (−)-Guaiol inhibits lung cancer EMT and IL-10 mediated STAT3 activation in vivo

To elucidate the relationship between (−)-Guaiol inhibiting EMT process of lung cancer and the STAT3 activation of macrophages in vivo, we detected the expression of EMT and STAT3 activation in macrophage depletion mice. (−)-Guaiol significantly suppressed EMT mRNA levels in mice without macrophage depletion, while the effects were partially or not compromised in macrophage depletion mice (Fig. 6A). Since IL-10 plays an important role in macrophage-mediated EMT, the levels of IL-10 secretion in peripheral blood of mice were measured. As shown in Fig. 6B. (−)-Guaiol substantially decreased IL-10 secretion in mice without macrophage depletion but not in the macrophage depletion mice. We verified EMT and STAT3 activation in mice without macrophage depletion. (−)-Guaiol weakened the EMT process and STAT3 phosphorylation compared with control. Moreover, the expression of CD206 and IL-10 as well as refrained by (−)-Guaiol (Fig. 6C).

In brief, the effect of (−)-Guaiol on lung cancer EMT process is, to some extent, mediated through IL-10/STAT3 signaling pathway.

4. Discussion

Macrophages are highly plastic immune cells in response to the located environment. The cross-talk between tumor cells and macrophages within the micro-environment contributes to cancer progression. Accumulated evidence demonstrated that the high expression of TAMs is negatively correlated with the prognosis of lung cancer patients [13,28]. Metastatic lesion exhibited elevated M2-like macrophage infiltration compared with primary lung tumors [29]. Targeting macrophage polarization is a potential therapeutic strategy in cancer therapy. In our present study, (−)-Guaiol showed an educate macrophage effect. By performing in vivo investigate in mouse model of macrophage depletion, (−)-Guaiol reduced the expression of M2-like macrophages in tumor tissue and spleen, but not the M1-like macrophages. In vitro study, we further verified the act of inhibiting manner to M2-like macrophages. In addition, we demonstrated (−)-Guaiol hold lung cancer growth in vivo, and prevent migration, invasion and EMT of lung cancer cells in co-culture. Interestingly, (−)-Guaiol exhibited active inhibitory function in lung cancer through suppressing M2-like macrophages either in vivo or in vitro studies.

Most of the function of TAMs attributes to secreting soluble factors which emitted by TAMs [30]. These TAMs-derived factors modulate the cross-talk between TAMs and lung cancer, as well as involve in the initiation and progression of EMT. Multiple cytokines and chemokines have been suggested to play a critical role as mediators of EMT process, including growth factors TGFβ, EGF [31,32], anti-inflammatory cytokine IL-10 [33], inflammatory cytokines IL-6, TNFα [34,35], chemokines CCL18, CCL22 [36–38], proteolytic enzyme MMPs [39]. Collectively, targeting these soluble factors could be the potential treatment strategies to interrupt the cross-talk between macrophages and EMT process of lung cancer. In accordance, integrating bioinformatics analysis provide evidence concerning the significance M2 macrophages in promoting lung cancer from functional genomic research angle. The enrichment analysis suggested that M2 secreted soluble factors as a critical lung cancer promotor by activating cytokines receptor signaling pathways. Here, we identified M2 secreted cytokines IL-10, IL-17, and IL-23 highly expressed in response to co-culture. Notably, only IL-10 secretion and mRNA expression were significantly decreased by (−)-Guaiol in co-culture. Our study revealed that IL-10 was a critical signaling molecule between macrophages and lung cancer cells for the anti-tumor effect of (−)-Guaiol.

Previous pieces of evidence suggested EMT associated phenotypes can be evoked by intracellular signaling pathways that are motivated when epithelial cells accept some specific signals from stromal microenvironment cells released [40]. New transcriptional procedures facilitate epithelial cells to mesenchymal changes [41], including deficiency of E-cadherin, acquisition of Vimentin, Fibronectin, N-cadherin, and overexpression of transcription factors Snail, Slug, Twist and Zeb1/2. Cytokines bind to their receptors trigger the phosphorylation and activation of Janus kinases (JAKs) and signal transducer and activator of transcription proteins (STATs); STAT dimers activate leading to induction of EMT in cancers [42]. Suppressor of cytokine limited EMT via JAK/STAT3 pathway in lung carcinoma [43,44]. Secretion of M2 macrophage-derived IL-10 could be induced by lung cancer cells [45–48]. In our vitro co-culture assay, we demonstrated that M2 macrophage-derived IL-10 facilitating STAT3 phosphorylation and activating EMT. In accordance, the systemic depletion of IL-10 (AS 101, IL-10 antagonist) leads to suppression of STAT3 phosphorylation and reversion of EMT. These results suggest the STAT3 signaling pathway involved in IL-10 mediated EMT in lung cancer. Notably, the activation of STAT3 and EMT was attenuated when LLC cells were treated by (−)-Guaiol in co-culture. Similar results were observed in vivo macrophage depleted mice model. After 3 weeks treatment of (−)-Guaiol, the expression of IL-10 level was decreased in peripheral blood. Simultaneously, STAT3 phosphorylation and EMT were suppressed in subcutaneous tumor of lung cancer. Taken together, it could be considered (−)-Guaiol disturbing the IL-10 regulated STAT3 signaling pathway.

In summary, we demonstrated that (−)-Guaiol, as an inhibitor of M2 macrophages, was validated an EMT reversed role possibly by targeting IL-10 to mediate STAT3 activation in vitro and in vivo assay. For the first time, our studies demonstrated that (−)-Guaiol plays a vital role in educating macrophages. We put our emphasis on understanding the inhibition effects of (−)-Guaiol on M2 macrophages. Our results propose a potential approach on lung cancer therapy by combining the plasticity of macrophages with anti-tumor effect of (−)-Guaiol.

There is a “paracrine feedback loop” to explain how lung cancer cells to induce M2 macrophages to secrete pro-tumor cytokines. However, we here should point out that polarization of macrophages is a complex process with multiple cytokines, chemokines, and growth factors secreted by macrophages and cancer cells [49,50]. Thus, it is worth in-depth identifying and targeting such cross-talk,

which represents a potential immunotherapeutic strategy for lung cancer. Future research endeavors ought to explore the regulatory relationship between (−)-Guaiol and other immune cells after the clearance of M2 macrophages.

5. Conclusions

In conclusion, our data suggested that (−)-Guaiol is a potential suppressor in M2 macrophages. IL-10, as the critical signaling molecule between M2 macrophages and lung cancer cells, can be blocked by (−)-Guaiol. EMT reverse effects of (−)-Guaiol were represented in the ability to prevent STAT3 activation through decreasing M2-derived IL-10. All of results in this study propose (−)-Guaiol can be a potential immune therapeutic candidate for the treatment of lung cancer.

Author contributions

Yajuan Cao; Yonghui Wu; Hongbin Tu: Conceived and designed the experiments; Performed the experiments; Analyzed and interpreted the data; Wrote the paper.

Zhan Gu; Fengzhi Yu; Weiling Huang; Shen Liping: Contributed reagents, materials, analysis tools or data.

Lixin Wang; Yan Li: Contributed reagents, materials, analysis tools or data; Wrote the paper.

Data availability statement

Data included in article/supp. material/referenced in article.

Ethics statement

The study was conducted in accordance with the Declaration of Helsinki and was approved by the Ethics Committee and the Institutional Review Board. The Ethics Committee of the Laboratory Animal Center of Tongji University School of Medicine approved the protocol with the ethics number TJAA11321101.

Declaration of competing interest

The authors declare that they have no known competing financial interests or personal relationships that could have appeared to influence the work reported in this paper.

Acknowledgements

This research was financially supported by Shanghai TCM Three-year action Plan TCM clinical key specialty cultivation project (ZY-FWTX-7001), Shanghai Science and Technology Commission Guide Science and Technology Support Project (18401901500), Shanghai Shenkang Center clinical Science and technology Innovation project (SHDC12018X20), the China Postdoctoral Science Foundation (Grant No. 2022M712405), and Shanghai Sailing Program (22YF1451400). China Postdoctoral Science Foundation (2021M701407) ; postdoctoral Innovation Project of Shandong Province (SDCX-ZG-202202005).

Appendix A. Supplementary data

Supplementary data to this article can be found online at https://doi.org/10.1016/j.heliyon.2023.e19817.

References

[1] F. Bray, J. Ferlay, I. Soerjomataram, R.L. Siegel, L.A. Torre, A. Jemal, Global cancer statistics 2018: globocan estimates of incidence and mortality worldwide for 36 cancers in 185 countries, CA Cancer J Clin 68 (6) (2018) 394–424, https://doi.org/10.3322/caac.21492.

[2] L.A. Torre, F. Bray, R.L. Siegel, J. Ferlay, J. Lortet-Tieulent, A. Jemal, Global cancer statistics, CA Cancer J Clin 65 (2) (2012) 87–108, https://doi.org/10.3322/caac.21262, 2015.

[3] D. Hanahan, R.A. Weinberg, Hallmarks of cancer: the next generation, Cell 144 (5) (2011) 646–674, https://doi.org/10.1016/j.cell.2011.02.013.

[4] J.E. Talmadge, I.J. Fidler, Aacr centennial series: the biology of cancer metastasis: historical perspective, Cancer Res. 70 (14) (2010) 5649–5669, https://doi.org/10.1158/0008-5472.CAN-10-1040.

[5] K.T. Yeung, J. Yang, Epithelial-mesenchymal transition in tumor metastasis, Mol. Oncol. 11 (1) (2017) 28–39, https://doi.org/10.1002/1878-0261.12017.

[6] N.M. Aiello, T. Brabletz, Y. Kang, M.A. Nieto, R.A. Weinberg, B.Z. Stanger, Upholding a role for emt in pancreatic cancer metastasis, Nature 547 (7661) (2017) E7–E8, https://doi.org/10.1038/nature22963.

[7] L. Prudkin, D.D. Liu, N.C. Ozburn, M. Sun, C. Behrens, X. Tang, K.C. Brown, B.N. Bekele, C. Moran, I.I. Wistuba, Epithelial-to-mesenchymal transition in the development and progression of adenocarcinoma and squamous cell carcinoma of the lung, Mod. Pathol. 22 (5) (2009) 668–678, https://doi.org/10.1038/modpathol.2009.19.

[8] X. Yan, L. Yan, S. Liu, Z. Shan, Y. Tian, Z. Jin, N-cadherin, a novel prognostic biomarker, drives malignant progression of colorectal cancer, Mol. Med. Rep. 12 (2) (2015) 2999–3006, https://doi.org/10.3892/mmr.2015.3687.

[9] X. Ye, T. Brabletz, Y. Kang, G.D. Longmore, M.A. Nieto, B.Z. Stanger, J. Yang, R.A. Weinberg, Upholding a role for emt in breast cancer metastasis, Nature 547 (7661) (2017) E1–E3, https://doi.org/10.1038/nature22816.

[10] M.R. Junttila, F.J. de Sauvage, Influence of tumour micro-environment heterogeneity on therapeutic response, Nature 501 (7467) (2013) 346–354, https://doi.org/10.1038/nature12626.

[11] K. Sawa-Wejksza, M. Kandefer-Szerszen, Tumor-associated macrophages as target for antitumor therapy, Arch. Immunol. Ther. Exp. 66 (2) (2018) 97–111, https://doi.org/10.1007/s00005-017-0480-8.

[12] D.M. Mosser, J.P. Edwards, Exploring the full spectrum of macrophage activation, Nat. Rev. Immunol. 8 (12) (2008) 958–969, https://doi.org/10.1038/nri2448.

[13] S. Gordon, F.O. Martinez, Alternative activation of macrophages: mechanism and functions, Immunity 32 (5) (2010) 593–604, https://doi.org/10.1016/j.immuni.2010.05.007.

[14] L. Yang, Y. Zhang, Tumor-associated macrophages: from basic research to clinical application, J. Hematol. Oncol. 10 (1) (2017) 58, https://doi.org/10.1186/s13045-017-0430-2.

[15] H. Li, N. Huang, W. Zhu, J. Wu, X. Yang, W. Teng, J. Tian, Z. Fang, Y. Luo, M. Chen, Y. Li, Modulation the crosstalk between tumor-associated macrophages and non-small cell lung cancer to inhibit tumor migration and invasion by ginsenoside rh2, BMC Cancer 18 (1) (2018) 579, https://doi.org/10.1186/s12885-018-4299-4.

[16] Z. Shu, J. Pu, L. Chen, Y. Zhang, K. Rahman, L. Qin, C. Zheng, Alisma orientale: ethnopharmacology, phytochemistry and pharmacology of an important traditional Chinese medicine, Am. J. Chin. Med. 44 (2) (2016) 227–251, https://doi.org/10.1142/S0192415X16500142.

[17] Q. Yang, J. Wu, Y. Luo, N. Huang, N. Zhen, Y. Zhou, F. Sun, Z. Li, Q. Pan, Y. Li, (-)-guaiol regulates rad51 stability via autophagy to induce cell apoptosis in non-small cell lung cancer, Oncotarget 7 (38) (2016) 62585–62597, https://doi.org/10.18632/oncotarget.11540.

[18] X. Yang, J. Zhu, J. Wu, N. Huang, Z. Cui, Y. Luo, F. Sun, Q. Pan, Y. Li, Q. Yang, (-)-guaiol regulates autophagic cell death depending on mtor signaling in nsclc, Cancer Biol. Ther. 19 (8) (2018) 706–714, https://doi.org/10.1080/15384047.2018.1451277.

[19] Y. Cao, W. Zhu, W. Chen, J. Wu, G. Hou, Y. Li, Prognostic value of birc5 in lung adenocarcinoma lacking egfr, kras, and alk mutations by integrated bioinformatics analysis, Dis. Markers (2019) (2019), 5451290, https://doi.org/10.1155/2019/5451290.

[20] V.K. Mootha, C.M. Lindgren, K.F. Eriksson, A. Subramanian, S. Sihag, J. Lehar, P. Puigserver, E. Carlsson, M. Ridderstrale, E. Laurila, N. Houstis, M.J. Daly, N. Patterson, J.P. Mesirov, T.R. Golub, P. Tamayo, B. Spiegelman, E.S. Lander, J.N. Hirschhorn, D. Altshuler, L.C. Groop, Pgc-1alpha-responsive genes involved in oxidative phosphorylation are coordinately downregulated in human diabetes, Nat. Genet. 34 (3) (2003) 267–273, https://doi.org/10.1038/ng1180.

[21] A. Subramanian, P. Tamayo, V.K. Mootha, S. Mukherjee, B.L. Ebert, M.A. Gillette, A. Paulovich, S.L. Pomeroy, T.R. Golub, E.S. Lander, J.P. Mesirov, Gene set enrichment analysis: a knowledge-based approach for interpreting genome-wide expression profiles, Proc Natl Acad Sci U S A 102 (43) (2005) 15545–15550, https://doi.org/10.1073/pnas.0506580102.

[22] H.Y. Tan, N. Wang, K. Man, S.W. Tsao, C.M. Che, Y. Feng, Autophagy-induced relb/p52 activation mediates tumour-associated macrophage repolarisation and suppression of hepatocellular carcinoma by natural compound baicalin, Cell Death Dis. 6 (10) (2015), e1942, https://doi.org/10.1038/cddis.2015.271.

[23] X. Dai, L. Lu, S. Deng, J. Meng, C. Wan, J. Huang, Y. Sun, Y. Hu, B. Wu, G. Wu, J.F. Lovell, H. Jin, K. Yang, Usp7 targeting modulates anti-tumor immune response by reprogramming tumor-associated macrophages in lung cancer, Theranostics 10 (20) (2020) 9332–9347, https://doi.org/10.7150/thno.47137.

[24] X. Zhang, L. Fan, J. Wu, H. Xu, W.Y. Leung, K. Fu, J. Wu, K. Liu, K. Man, X. Yang, J. Han, J. Ren, J. Yu, Macrophage p38alpha promotes nutritional steatohepatitis through m1 polarization, J. Hepatol. 71 (1) (2019) 163–174, https://doi.org/10.1016/j.jhep.2019.03.014.

[25] Q. Yang, J. Wu, Y. Luo, N. Huang, N. Zhen, Y. Zhou, F. Sun, Z. Li, Q. Pan, Y. Li, (-)-guaiol regulates rad51 stability via autophagy to induce cell apoptosis in non-small cell lung cancer, Oncotarget 7 (38) (2016) 62585–62597, https://doi.org/10.18632/oncotarget.11540.

[26] L. Yang, Y. Dong, Y. Li, D. Wang, S. Liu, D. Wang, Q. Gao, S. Ji, X. Chen, Q. Lei, W. Jiang, L. Wang, B. Zhang, J.J. Yu, Y. Zhang, Il-10 derived from m2 macrophage promotes cancer stemness via jak1/stat1/nf-kappab/notch1 pathway in non-small cell lung cancer, Int. J. Cancer 145 (4) (2019) 1099–1110, https://doi.org/10.1002/ijc.32151.

[27] S. Gao, J. Hu, X. Wu, Z. Liang, Pma treated thp-1-derived-il-6 promotes emt of sw48 through stat3/erk-dependent activation of wnt/beta-catenin signaling pathway, Biomed. Pharmacother. 108 (2018) 618–624, https://doi.org/10.1016/j.biopha.2018.09.067.

[28] L. Cao, X. Che, X. Qiu, Z. Li, B. Yang, S. Wang, K. Hou, Y. Fan, X. Qu, Y. Liu, M2 macrophage infiltration into tumor islets leads to poor prognosis in non-small-cell lung cancer, Cancer Manag. Res. 11 (2019) 6125–6138, https://doi.org/10.2147/CMAR.S199832.

[29] Y. Kudo, C. Haymaker, J. Zhang, A. Reuben, D.Y. Duose, J. Fujimoto, S. Roy-Chowdhuri, S.L. Solis, H. Dejima, E.R. Parra, B. Mino, R. Abraham, N. Ikeda, A. Vaporcyan, D. Gibbons, J. Zhang, F.F. Lang, R. Luthra, J.J. Lee, C. Moran, J.T. Huse, H. Kadara, I.I. Wistuba, Suppressed immune microenvironment and repertoire in brain metastases from patients with resected non-small-cell lung cancer, Ann. Oncol. 30 (9) (2019) 1521–1530, https://doi.org/10.1093/annonc/mdz207.

[30] O.W. Yeung, C.M. Lo, C.C. Ling, X. Qi, W. Geng, C.X. Li, K.T. Ng, S.J. Forbes, X.Y. Guan, R.T. Poon, S.T. Fan, K. Man, Alternatively activated (m2) macrophages promote tumour growth and invasiveness in hepatocellular carcinoma, J. Hepatol. 62 (3) (2015) 607–616, https://doi.org/10.1016/j.jhep.2014.10.029.

[31] Q.M. Fan, Y.Y. Jing, G.F. Yu, X.R. Kou, F. Ye, L. Gao, R. Li, Q.D. Zhao, Y. Yang, Z.H. Lu, L.X. Wei, Tumor-associated macrophages promote cancer stem cell-like properties via transforming growth factor-beta1-induced epithelial-mesenchymal transition in hepatocellular carcinoma, Cancer Lett. 352 (2) (2014) 160–168, https://doi.org/10.1016/j.canlet.2014.05.008.

[32] A. Nabeshima, Y. Matsumoto, J. Fukushi, K. Iura, T. Matsunobu, M. Endo, T. Fujiwara, K. Iida, Y. Fujiwara, M. Hatano, N. Yokoyama, S. Fukushima, Y. Oda, Y. Iwamoto, Tumour-associated macrophages correlate with poor prognosis in myxoid liposarcoma and promote cell motility and invasion via the hb-egf-egfr-pi3k/akt pathways, Br. J. Cancer 112 (3) (2015) 547–555, https://doi.org/10.1038/bjc.2014.637.

[33] L. Qi, H. Yu, Y. Zhang, D. Zhao, P. Lv, Y. Zhong, Y. Xu, Il-10 secreted by m2 macrophage promoted tumorigenesis through interaction with jak2 in glioma, Oncotarget 7 (44) (2016) 71673–71685, https://doi.org/10.18632/oncotarget.12317.

[34] D. Che, S. Zhang, Z. Jing, L. Shang, S. Jin, F. Liu, J. Shen, Y. Li, J. Hu, Q. Meng, Y. Yu, Macrophages induce emt to promote invasion of lung cancer cells through the il-6-mediated cox-2/pge(2)/beta-catenin signalling pathway, Mol. Immunol. 90 (2017) 197–210, https://doi.org/10.1016/j.molimm.2017.06.018.

[35] Y. Meng, M.A. Beckett, H. Liang, H.J. Mauceri, N. van Rooijen, K.S. Cohen, R.R. Weichselbaum, Blockade of tumor necrosis factor alpha signaling in tumor-associated macrophages as a radiosensitizing strategy, Cancer Res. 70 (4) (2010) 1534–1543, https://doi.org/10.1158/0008-5472.CAN-09-2995.

[36] J. Chen, Y. Yao, C. Gong, F. Yu, S. Su, J. Chen, B. Liu, H. Deng, F. Wang, L. Lin, H. Yao, F. Su, K.S. Anderson, Q. Liu, M.E. Ewen, X. Yao, E. Song, Ccl18 from tumor-associated macrophages promotes breast cancer metastasis via pitpnm3, Cancer Cell 19 (4) (2011) 541–555, https://doi.org/10.1016/j.ccr.2011.02.006.

[37] L. Gao, F.Q. Wang, H.M. Li, J.G. Yang, J.G. Ren, K.F. He, B. Liu, W. Zhang, Y.F. Zhao, Ccl2/egf positive feedback loop between cancer cells and macrophages promotes cell migration and invasion in head and neck squamous cell carcinoma, Oncotarget 7 (52) (2016) 87037–87051, https://doi.org/10.18632/oncotarget.13523.

[38] S. Lee, E. Lee, E. Ko, M. Ham, H.M. Lee, E.S. Kim, M. Koh, H.K. Lim, J. Jung, S.Y. Park, A. Moon, Tumor-associated macrophages secrete ccl2 and induce the invasive phenotype of human breast epithelial cells through upregulation of ero1-alpha and mmp-9, Cancer Lett. 437 (2018) 25–34, https://doi.org/10.1016/j.canlet.2018.08.025.

[39] X. Liu, Z. Lv, J. Zou, X. Liu, J. Ma, C. Sun, N. Sa, W. Xu, Elevated aeg-1 expression in macrophages promotes hypopharyngeal cancer invasion through the stat3-mmp-9 signaling pathway, Oncotarget 7 (47) (2016) 77244–77256, https://doi.org/10.18632/oncotarget.12886.

[40] A. Dongre, R.A. Weinberg, New insights into the mechanisms of epithelial-mesenchymal transition and implications for cancer, Nat. Rev. Mol. Cell Biol. 20 (2) (2019) 69–84, https://doi.org/10.1038/s41580-018-0080-4.

[41] T. Shibue, R.A. Weinberg, Emt, cscs, and drug resistance: the mechanistic link and clinical implications, Nat. Rev. Clin. Oncol. 14 (10) (2017) 611–629, https://doi.org/10.1038/nrclinonc.2017.44.

[42] G.S. Markopoulos, E. Roupakia, K.B. Marcu, E. Kolettas, Epigenetic regulation of inflammatory cytokine-induced epithelial-to-mesenchymal cell transition and cancer stem cell generation, Cells 8 (10) (2019), https://doi.org/10.3390/cells8101143.

[43] M. Shen, Z. Xu, W. Xu, K. Jiang, F. Zhang, Q. Ding, Z. Xu, Y. Chen, Inhibition of atm reverses emt and decreases metastatic potential of cisplatin-resistant lung cancer cells through jak/stat3/pd-l1 pathway, J. Exp. Clin. Cancer Res. 38 (1) (2019) 149, https://doi.org/10.1186/s13046-019-1161-8.
[44] Y. Zhou, Z. Zhang, N. Wang, J. Chen, X. Zhang, M. Guo, Z.L. John, Q. Wang, Suppressor of cytokine signalling-2 limits igf1r-mediated regulation of epithelial-mesenchymal transition in lung adenocarcinoma, Cell Death Dis. 9 (4) (2018) 429, https://doi.org/10.1038/s41419-018-0457-5.
[45] M. Tariq, J.Q. Zhang, G.K. Liang, Q.J. He, L. Ding, B. Yang, Gefitinib inhibits m2-like polarization of tumor-associated macrophages in lewis lung cancer by targeting the stat6 signaling pathway, Acta Pharmacol. Sin. 38 (11) (2017) 1501–1511, https://doi.org/10.1038/aps.2017.124.
[46] X. Hu, Y. Gu, S. Zhao, S. Hua, Y. Jiang, Increased il-10+cd206+cd14+m2-like macrophages in alveolar lavage fluid of patients with small cell lung cancer, Cancer Imm. Immunother. 69 (12) (2020) 2547–2560, https://doi.org/10.1007/s00262-020-02639-z.
[47] Z. Cheng, L. Wang, C. Wu, L. Huang, Y. Ruan, W. Xue, Tumor-derived exosomes induced m2 macrophage polarization and promoted the metastasis of osteosarcoma cells through tim-3, Arch. Med. Res. 52 (2) (2021) 200–210, https://doi.org/10.1016/j.arcmed.2020.10.018.
[48] L. Cui, G. Yang, J. Ye, Y. Yao, G. Lu, J. Chen, L. Fang, S. Lu, J. Zhou, Dioscin elicits anti-tumour immunity by inhibiting macrophage m2 polarization via jnk and stat3 pathways in lung cancer, J. Cell Mol. Med. 24 (16) (2020) 9217–9230, https://doi.org/10.1111/jcmm.15563.
[49] A. Salmaninejad, S.F. Valilou, A. Soltani, S. Ahmadi, Y.J. Abarghan, R.J. Rosengren, A. Sahebkar, Tumor-associated macrophages: role in cancer development and therapeutic implications, Cell. Oncol. 42 (5) (2019) 591–608, https://doi.org/10.1007/s13402-019-00453-z.
[50] A. Shapouri-Moghaddam, S. Mohammadian, H. Vazini, M. Taghadosi, S.A. Esmaeili, F. Mardani, B. Seifi, A. Mohammadi, J.T. Afshari, A. Sahebkar, Macrophage plasticity, polarization, and function in health and disease, J. Cell. Physiol. 233 (9) (2018) 6425–6440, https://doi.org/10.1002/jcp.26429.